Astron. Astrophys. 317, 90–98 (1997)

ASTRONOMY
AND
ASTROPHYSICS

A theoretical approach to globular cluster low main sequence stars

D.R. Alexander[1], **E. Brocato**[2], **S. Cassisi**[2,3], **V. Castellani**[2,4,5], **F. Ciacio**[6], **and S. Degl'Innocenti**[6,7]

[1] Physics Department, Wichita State University, Wichita KS67260, USA
[2] Osservatorio Astronomico di Collurania, Via M. Maggini, I-64100 Teramo, Italy
[3] Dipartimento di Fisica, Università dell'Aquila, Via Vetoio, I-67100 L'Aquila, Italy
[4] Dipartimento di Fisica, Università di Pisa, Piazza Torricelli 2, I-56100 Pisa, Italy
[5] INFN Lab. Naz. Gran Sasso, I-67100 L'Aquila, Italy
[6] INFN Sezione di Ferrara I-44100 Ferrara, Italy
[7] Max-Planck Institut fur Astrophysics, K. Schwarzschild Str. 1, D-85740 Garching bei Munchen, Germany

Received 6 November 1995 / Accepted 21 May 1996

Abstract. This paper present new evolutionary computations extending toward the lower main sequence previous computations given for globular cluster stars. We discuss the physical inputs with particular regard to the limit of the adopted usual treatment of the stellar atmosphere, which allows a tight correlation with actual stellar structures only for selected range of masses, depending on the assumed metallicity. Theoretical evolutionary properties of Very Low Mass (VLM) stars are presented and discussed. We find that adopting new extended tabulations of radiative opacity, as computed according to Alexander & Fergusson (1994) procedures and by relying on the Saumon & Chabrier (1992) equation of state (EOS) our results allow a reasonable fitting of HST observation of metal poor VLM objects in the galactic globular NGC 6397. The investigation has been extended to a sample of field VLM star with known parallaxes, showing again a satisfactory agreement with the distribution of metal poor dwarfs and discussing the present theoretical scenario for solar metallicity VLM. Selected evolutionary quantities are presented in suitable tables for metal poor objects (Y=0.23, Z=0.0001, 0.0003, 0.0006 and 0.001). A brief discussion including a comparison of mass-luminosity relations for VLM objects for the various investigated metallicities closes the paper.

Key words: stars: evolution – stars: Hertzsprung-Russel diagram – stars: population II – globular clusters: general – stars: low-mass, subdwarfs

Send offprint requests to: V. Castellani, Dipartimento di Fisica Universita' di Pisa, Piazza Torricelli 2, I-56100 Pisa, Italy

1. Introduction

The improved efficiency of the Hubble Space Telescope is opening to the investigation the still unexplored field of very faint stars in galactic globular clusters at last. According to long debated expectations (see, e.g., Castellani 1979), now deep CM diagrams are disclosing the evidence for the sequence of cooling white dwarfs, extending in the same time our knowledge of main sequence stars down to about their natural limit, i.e., towards the lower mass limit for the ignition of nuclear H burning in the structures.

In a series of previous papers we presented theoretical computations covering the evolution of globular cluster stars from the phases of central H burning up to the final cooling as White Dwarfs (see, e.g., Castellani et al. 1989, Castellani et al. 1994 and references therein). According to new observational evidence, in this paper evolutionary computations devoted to extend previous evaluations to less massive stars will be presented, in order to implement - as far as possible- the theoretical scenario with suitable evaluations for stars well below the Turn-Off, along the cluster main sequence.

The physical inputs of present computations will be discussed in the next section. Section 3 will deal with the theoretical evolutionary behavior of very low mass (VLM) models, discussing some features which have received scarce attention in the previous literature and which could be of interest for people concerned with the theory of stellar structures. In the next section (Sect. 4) the evolutionary results regarding the lower main sequence of metal poor structures, will be presented comparing theoretical data with HST observations of the galactic globular NGC 6397. The evolutionary scenario for the sequence of dwarfs with known parallaxes, will be finally revisited, shortly discussing metal rich VLM structures. tables of selected evolutionary data will be provided both in the theoretical and in the

observational (M_V, V-I) plane, to be used for comparison with previous work on the argument and with observational data.

2. The physical inputs

Since the pioneering work by Limber (1958) investigations given by several authors have already brought to light a series of happy features characterizing the structure of very low mass (VLM) stars. VLM stars appear rather insensitive to two evolutionary parameters which affect the structures of more massive stars, namely the mixing length parameter and the amount of original He (see e.g. Vanderberg et al. 1983). Unfortunately, when entering the range of VLM cool stars the theoretical evaluations about these structures are critically dependent on the difficult evaluation of both the opacity and the equation of state for a cool gas, where molecules and grains play a relevant role. Interested readers can find a detailed discussion about this last point in Dorman et al. (1989).

As for low temperature opacities, tabulations available in the literature including molecules and grains, as presented by Alexander et al. (1983, 1989) and Alexander & Ferguson (1994) were found not to cover the whole range of pressure experienced by a VLM star, thus requiring more or less tentative extrapolations. A new extended tabulation has been computed for this project, allowing a full coverage of VLM structures for selected choices about the star metallicity. We expect that such new evaluations should maintain validity for densities lower or of the order of 0.01 gr/cm^3, a range which appears fully adequate for our purposes.

Low temperature opacities were implemented at T$>$ 10000^{o}K with radiative opacities by Roger & Iglesias (1992) (OPAL), as made available at the anonymous ftp account. When necessary, this last tabulation was further integrated with opacity values from the Los Alamos Opacity Library (Huebner et al. 1977), computed for the same mixture (Grevesse 1991) of the OPAL and Alexander & Ferguson opacity tables. In all cases, this occurs at large values of temperature and density, where Los Alamos opacities nicely overlap OPAL predictions.

As already indicated, the second critical ingredient for the theory of VLM structures is given by the appropriate evaluation of the EOS for similar dense and cool objects. Courtesy of dr. Chabrier, we were enabled to insert in our evolutionary code the most recent EOS evaluated adopting a free-energy minimization technique (Saumon & Chabrier 1992, Saumon et al. 1995) for a zero metal mixture. According to a well established scenario, the presence of metals should play little or no role in the EOS up to metal contents of the order of the solar metallicity (see, e.g. Hubbard 1994). However, we will mainly refer to computations in the range Z= 0.0001-0.001 which appear suitable for the large majority of galactic globular clusters and, in the same time, should allow a safe use of the zero metal EOS.

With the above quoted assumptions, present computations appear based on the most updated physics presently available. However, VLM stars present another difficulty as given by the treatment of stellar atmospheres. As it has been widely debated (see, e.g., Baraffe et al. 1995 and reference therein) in solar metallicity models below about T_{eff} = 4000K (and down to about 2500K) the Eddington approximation and, thus, the $T(\tau)$ relation is expected to become unrealistic. According to Burrows et al. (1993) this limits increases above $T_{eff} \sim 4500K$ ($logT_e \sim 3.65$) decreasing the star metallicity down to the extreme case Z=0. Because of the lack of suitable model atmospheres, we were forced to neglect such an occurrence. Atmospheric integrations where thus performed adopting the Krishna-Swamy (1966) solar scaled $T(\tau)$ formula until reaching $\tau = 2/3$ or, alternatively, until the onset of convection, where mixing length has been used to evaluate the degree of superadiabaticity. Comparison of models in Burrows et al. (1989, 1993: but see also Fig. 2 in Baraffe et al. (1995)) discloses that in quoted range of temperature our models should tend to be a bit hotter and more luminous than expected on the basis of a proper treatment of the atmosphere.

According to such an evidence, present results can be regarded as an investigation on the effect of updating the physical input (EOS and opacity) in previous results appeared in the literature, as based on similar assumptions about the treatment of the atmospheric layers (as in Dorman et al. 1989, D'Antona & Mazzitelli 1994, 1996). However, as it will be discussed later on, even restricting the investigation to the range of validity of $T(\tau)$ one can significatively extend previous computations into the range of very low stellar masses. Moreover, it appears that the HR diagram location of the sequence of VLM models is not dramatically affected by the release of Eddington approximation, so that the use of a $T(\tau)$ relation can be regarded at least as a first order approximation to the expected models behavior.

3. Theoretical VLM stellar structures

Selected sequences of metal poor stellar models have been computed to cover the range of H burning stars below M = 0.8$M_\odot$, assuming Y=0.23 everywhere. In this section we will discuss some structural evolutionary features of the computed models which represent a common feature for all VLM structures independently of the assumed amount of metal and/or the treatment of stellar atmospheres. According to the calibration of solar models, all computations assume a mixing length parameter as given by α=2.2. However, numerical experiments confirmed that below, about, M=0.5 M$_\odot$ varying the assumption on the mixing length within reasonable limit ($1.5 \leq \alpha \leq 2.5$) or varying Y within ΔY $\approx \pm$ 0.02 have quite a negligible influence on the results. All models have been followed from an early pre-main sequence phase till, at least, an age of 20 Gyr. Selected models have been followed till the last phases of exhaustion of central H, often for a time much larger than the Hubble time. Of course, in this way stellar structures that will populate the Universe only in an extremely far future, have been computed. However, similar unrealistic models have been used to learn some interesting features of the VLM evolutionary scenario that we will discuss here in the following.

As well known, when reaching the range of VLM structures, the common notion of Zero Age Main Sequence, as given by

Table 1. Selected evolutionary quantities (see text) for VLM stellar structures.

$M/M_\odot$	$\log t_H$	$\log t_{nucl}$	$\log t_{(^3He)}$	X/X_{in}	$(^3He)^{eq}$	*H burning structure*
0.70	10.4	7.5	7.5	1.00	$3 \cdot 10^{-4}$	*Convective core*
0.60	10.6	7.7	7.7	1.00	$6 \cdot 10^{-4}$	" "
0.50	10.9	8.0	8.5	0.99	$1 \cdot 10^{-3}$	" "
0.40	11.2	8.2	9.2	0.97	$3 \cdot 10^{-3}$	" "
0.30	11.6	8.5	10.2	0.95	$7 \cdot 10^{-3}$	*Fully convective*
0.20	11.9	8.6	10.7	0.94	$2 \cdot 10^{-2}$	" "
0.15	12.1	8.7	11.1	0.90	$4 \cdot 10^{-2}$	" "

structures where secondary elements in H burning already attained their equilibrium values, becomes more and more meaningless since ^3He behaves as a pseudo primary element, with a lifetime becoming comparable to the lifetime for central H burning, so that models start depleting H with ^3He still well below its equilibrium value. This is shown in Table 1 where for selected values of stellar masses the typical time spent by the structures burning H (t_H), the age at which the contribution of gravitational energy vanishes (t_{nucl}), the age of the models attaining ^3He equilibrium ($t_{^3He}$), the ratio between the amount of H at the center of this model and the initial H abundance, and the abundance by mass of ^3He at the equilibrium, are reported. However, the same table shows that after 1 Gyr the structures are in all cases already supported by nuclear burning only, placed on what we can regard as the initial Main Sequence location. Last column in Table 1 reports the convective structure of these models. As already known, below about $M \simeq 0.3M_\odot$ only fully convective stellar structures, with a progressive amount of electronic degeneracy which, eventually, succeeds in inhibiting the release of gravitational heating and the ignition of central H nuclear burning, are found. Top and bottom panels of Fig. 1 disclose the time behavior of selected structural parameters for two models with 0.4 and $0.3M_\odot$, respectively. The $0.4M_\odot$ model behaves like the well known models with moderately larger masses populating the upper portion of the cluster main sequence. The increase of ^3He toward its equilibrium value increases the efficiency of the burning and the structure reacts decreasing both central temperature and density, which start increasing again only when the equilibrium value for ^3He has been attained. However, fully convective structures behave quite differently, and central density keeps decreasing all along the major phase of H burning. A similar steady decrease of central density is a well known feature but not yet discussed of the He burning ignition in the center of more massive stars.

According to plain mathematical elaborations, one finds that the curious behavior of VLM fully convective structures is just the one expected in homological models with increasing molecular weight. As a matter of the fact, as shown in the same Fig. 1, one finds that the central density of the $0.3M_\odot$ model starts suddenly increasing again in the very last phases of central H burning, when the increased abundance of He and the corresponding decrease of radiative opacities induces a radiative shell which rapidly grows to eventually form a radiative core. Further details on the argument, as well as a detailed description of VLM evolutionary features, can be found in Ciacio (1994).

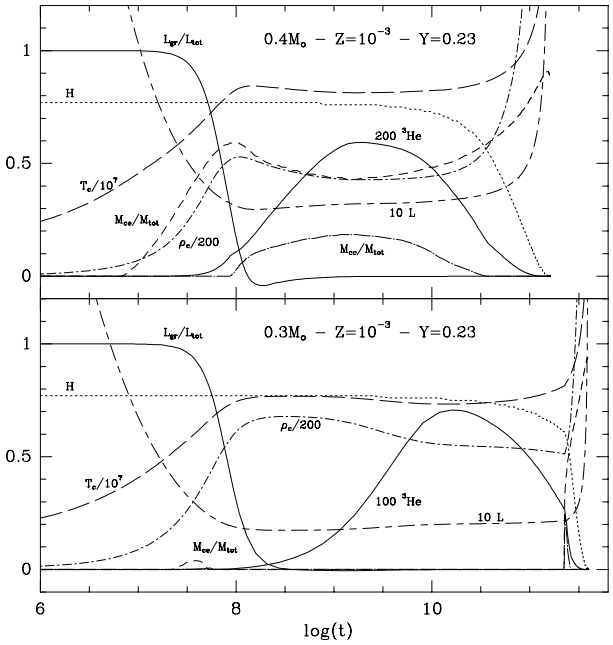

Fig. 1. The variation with time of stellar luminosity (L) in solar unit, contribution of gravitation to the total luminosity (L_{grav}/L_{tot}), central density (ρ_c), central temperature (T_c), size of the convective core (M_{cc}) as fraction of the total mass, mass location of the bottom of the convective envelope (M_{ce}), and central abundances by mass of H and ^3He for models with M = $0.4M_\odot$ (top panel) and M = $0.3M_\odot$ (lower panel) with Z = 10^{-3}, Y = 0.23.

Fig. 2 shows the effect of age on the HR diagram distribution of a typical set of models. Data in this figure are presented as an example of evolutionary effects, showing that in "not-too-young" VLM stellar systems, the age plays a negligible role on the HR diagram location of stars below, about $0.5M_\odot$. Interesting enough, the $0.3M_\odot$ model appears the less affected by age, less massive models shoving a progressively increasing sensitivity to the adopted ages. The reason for such a behavior is disclosed by Fig. 3, where the variation with time of the amount of central ^3He for selected choices about the stellar mass, has been reported. It appears that in the $0.3M_\odot$ case, at t=10 Gyr central ^3He has already approached its equilibrium value, so that the following evolution is governed by the depletion of central H only. On the contrary, less massive models keep increasing central ^3He, thus increasing the efficiency of proton-proton burning and readjusting the structure according to such an occurrence. A readjustment that in the less massive models is amplified by the decreasing electronic degeneracy induced by the decrease of central density.

4. Metal poor VLM main sequences

Tables 2 to 5 give selected theoretical quantities for models with $M \leq 0.6M_\odot$ for four selected choices about the heavy metal content (Z=0.0001, Z= 0.0003, Z=0.0006, Z=0.001) and for the labeled assumptions about star masses and ages. In the same tables, there are also the expected location in the (V, V-I) obser-

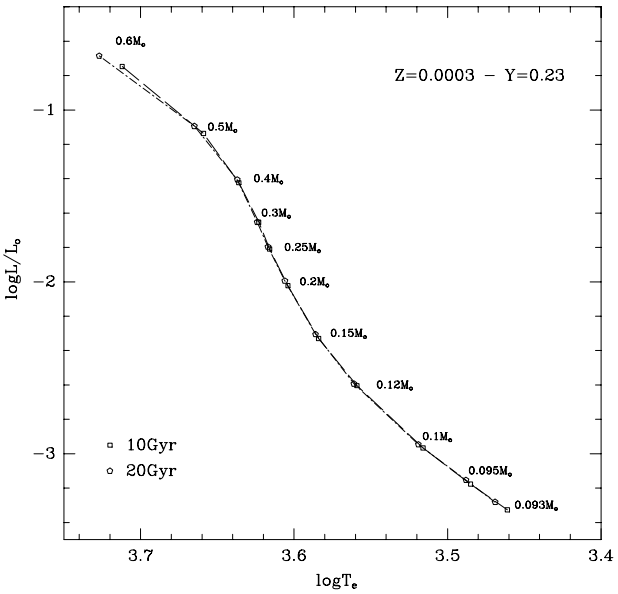

Fig. 2. The evolution with time of the HR diagram location of models with Z=0.0003 for the labeled assumptions on the cluster age.

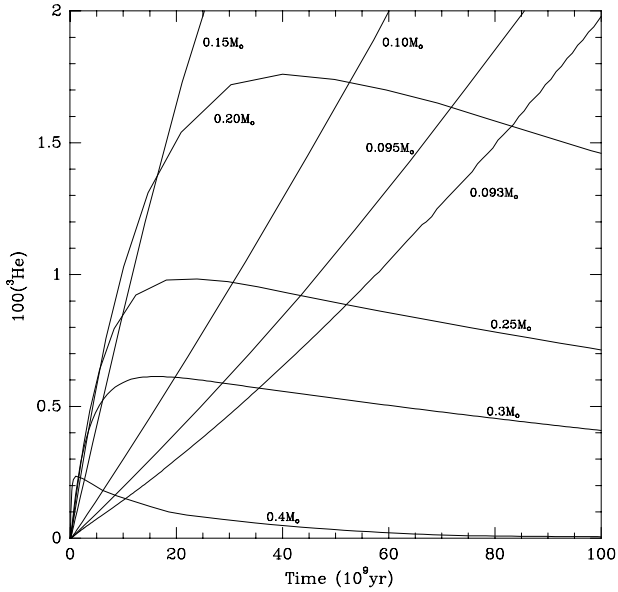

Fig. 3. The behavior with time of the abundance by mass of central ^3He for the labeled assumptions about the stellar masses and for Z=0.0003 - Y=0.23.

vational plane, as evaluated adopting bolometric correction and color temperature relation from Kurucz (1993) implemented for effective temperatures lower than $4000K$ with similar evaluations given by Allard & Hauschildt (1995) shifted to overlap Kurucz evaluation at the fitting point ($T \approx 4000K$) (see the discussion in D'Antona & Mazzitelli 1996, hereafter DM96).

Fig. 4 reports the location of the 10 Gyr sequences in the theoretical HR diagram for the four choices on the star metallicity. From this figure it is possible to recognize the already known sinuous shape of the VLM sequence together with the

Table 2. Luminosity, effective temperature, surface gravity, central density and temperature and the expected location in the (M_V,V-I) observational plane, for stellar models with $M \leq 0.6M_\odot$ with metallicity $Z = 10^{-4}$ and $Y = 0.23$, at ages equal to 10 Gyr and 20 Gyr.

$M/M_\odot$		$\log(L/L_\odot)$	$\log T_e$	$\log g$	$\log \rho_c$	$\log T_c$	M_V	$(V-I)$
0.6	$10Gyr$	-0.735	3.719	4.774	1.775	7.006	6.924	0.963
	$20Gyr$	-0.679	3.733	4.774	1.772	7.009	6.759	0.906
0.5	$10Gyr$	-1.090	3.674	4.869	2.029	6.973	7.952	1.175
	$20Gyr$	-1.037	3.680	4.840	2.135	6.996	7.795	1.144
0.4	$10Gyr$	-1.376	3.652	4.970	1.978	6.930	8.774	1.299
	$20Gyr$	-1.359	3.653	4.957	2.036	6.939	8.725	1.293
0.3	$10Gyr$	-1.602	3.641	5.028	2.061	6.879	9.408	1.371
	$20Gyr$	-1.598	3.641	5.024	2.056	6.880	9.398	1.371
0.25	$10Gyr$	-1.754	3.633	5.068	2.161	6.852	9.838	1.421
	$20Gyr$	-1.742	3.634	5.060	2.148	6.851	9.802	1.415
0.20	$10Gyr$	-1.966	3.621	5.135	2.308	6.820	10.463	1.503
	$20Gyr$	-1.942	3.622	5.115	2.279	6.817	10.394	1.495
0.15	$10Gyr$	-2.277	3.599	5.233	2.523	6.770	11.429	1.656
	$20Gyr$	-2.251	3.602	5.219	2.498	6.770	11.342	1.635
0.12	$10Gyr$	-2.558	3.575	5.322	2.688	6.707	12.293	1.817
	$20Gyr$	-2.543	3.577	5.315	2.677	6.713	12.242	1.804
0.10	$10Gyr$	-2.939	3.528	5.435	2.903	6.616	13.499	2.114
	$20Gyr$	-2.918	3.532	5.430	2.892	6.622	13.431	2.091
0.097	$10Gyr$	-3.066	3.510	5.477	2.973	6.583	13.881	2.220
	$20Gyr$	-3.042	3.514	5.469	2.960	6.590	13.807	2.197
0.096	$10Gyr$	-3.129	3.501	5.500	3.007	6.565	14.067	2.274
	$20Gyr$	-3.099	3.506	5.490	2.990	6.575	13.976	2.244

Table 3. As in Table 1, but for a metallicity $Z = 3 \cdot 10^{-4}$.

$M/M_\odot$		$\log(L/L_\odot)$	$\log T_e$	$\log g$	$\log \rho_c$	$\log T_c$	M_V	$(V-I)$
0.6	$10Gyr$	-0.747	3.712	4.758	1.782	7.006	6.960	0.986
	$20Gyr$	-0.685	3.727	4.760	1.776	7.009	6.781	0.924
0.5	$10Gyr$	-1.137	3.659	4.856	2.018	6.966	8.148	1.256
	$20Gyr$	-1.094	3.665	4.837	2.098	6.983	8.009	1.221
0.4	$10Gyr$	-1.423	3.636	4.953	1.970	6.923	9.004	1.409
	$20Gyr$	-1.405	3.637	4.939	2.018	6.930	8.952	1.402
0.3	$10Gyr$	-1.653	3.623	5.007	2.033	6.870	9.678	1.501
	$20Gyr$	-1.652	3.624	5.010	2.036	6.872	9.666	1.494
0.25	$10Gyr$	-1.809	3.616	5.055	2.142	6.847	10.133	1.554
	$20Gyr$	-1.796	3.617	5.046	2.127	6.845	10.092	1.547
0.20	$10Gyr$	-2.022	3.604	5.123	2.293	6.816	10.775	1.644
	$20Gyr$	-1.994	3.606	5.103	2.262	6.812	10.687	1.629
0.15	$10Gyr$	-2.329	3.584	5.225	2.506	6.766	11.693	1.783
	$20Gyr$	-2.305	3.586	5.209	2.479	6.766	11.619	1.769
0.12	$10Gyr$	-2.604	3.559	5.304	2.665	6.704	12.561	1.953
	$20Gyr$	-2.593	3.561	5.301	2.657	6.708	12.519	1.939
0.10	$10Gyr$	-2.966	3.516	5.414	2.866	6.618	13.771	2.268
	$20Gyr$	-2.946	3.519	5.406	2.855	6.624	13.700	2.245
0.095	$10Gyr$	-3.177	3.485	5.479	2.975	6.566	14.527	2.525
	$20Gyr$	-3.153	3.488	5.467	2.963	6.572	14.444	2.498
0.093	$10Gyr$	-3.327	3.461	5.524	3.050	6.525	15.264	2.794
	$20Gyr$	-3.281	3.469	5.510	3.028	6.538	15.004	2.694

effect of metallicity on the HR diagram location, so by increasing the metallicity for each given value of the mass, cooler and moderately less luminous structures are being expected. For the sake of comparison, in the same figure the location of a Z=0.006 sequence has been added, which however has to be regarded with caution, since it is difficult to evaluate if metals begin to play a not marginal role in the EOS of such a moderately metal rich mixture. According to the discussion given in Sect. 2, the same figure shows at $\log T_e$=3.60 or 3.65 the lower temperature limit for the validity of the adopted treatment of stellar atmospheres either in the solar or in the zero metal case, respectively. Present results can be usefully compared with similar results recently presented by DM96 for Z=0.0001, Z=0.001.

Table 4. As in Table 1, but for a metallicity $Z = 6 \cdot 10^{-4}$.

$M/M_\odot$		$\log(L/L_\odot)$	$\log T_e$	$\log g$	$\log \rho_c$	$\log T_c$	M_V	$(V-I)$
0.6	$10Gyr$	-0.763	3.705	4.746	1.790	7.006	7.013	1.010
	$20Gyr$	-0.702	3.721	4.749	1.781	7.008	6.815	0.941
0.5	$10Gyr$	-1.143	3.650	4.826	2.015	6.965	8.225	1.315
	$20Gyr$	-1.091	3.656	4.798	2.109	6.985	8.058	1.275
0.4	$10Gyr$	-1.457	3.625	4.943	1.969	6.917	9.187	1.500
	$20Gyr$	-1.438	3.626	4.928	2.019	6.925	9.129	1.491
0.3	$10Gyr$	-1.688	3.613	5.002	2.023	6.866	9.875	1.595
	$20Gyr$	-1.687	3.614	5.005	2.023	6.868	9.863	1.587
0.25	$10Gyr$	-1.850	3.605	5.052	2.138	6.846	10.354	1.658
	$20Gyr$	-1.834	3.606	5.040	2.119	6.843	10.305	1.650
0.20	$10Gyr$	-2.061	3.594	5.122	2.288	6.814	10.972	1.738
	$20Gyr$	-2.035	3.595	5.100	2.257	6.810	10.899	1.731
0.15	$10Gyr$	-2.366	3.572	5.214	2.492	6.762	11.901	1.888
	$20Gyr$	-2.346	3.574	5.202	2.471	6.763	11.836	1.874
0.12	$10Gyr$	-2.638	3.548	5.294	2.649	6.702	12.780	2.066
	$20Gyr$	-2.627	3.550	5.291	2.641	6.706	12.736	2.051
0.10	$10Gyr$	-2.986	3.507	5.398	2.841	6.620	14.043	2.428
	$20Gyr$	-2.971	3.509	5.391	2.833	6.625	13.985	2.409
0.097	$10Gyr$	-3.087	3.492	5.426	2.891	6.596	14.467	2.588
	$20Gyr$	-3.070	3.495	5.421	2.883	6.600	14.390	2.556
0.095	$10Gyr$	-3.174	3.479	5.452	2.931	6.575	14.857	2.744
	$20Gyr$	-3.156	3.481	5.442	2.924	6.579	14.788	2.721
0.093	$10Gyr$	-3.300	3.459	5.489	2.995	6.543	15.603	3.046
	$20Gyr$	-3.276	3.463	5.481	2.983	6.550	15.464	2.983

Table 5. As in Table 1, but for a metallicity $Z = 10^{-3}$.

$M/M_\odot$		$\log(L/L_\odot)$	$\log T_e$	$\log g$	$\log \rho_c$	$\log T_c$	M_V	$(V-I)$
0.6	$10Gyr$	-0.782	3.697	4.733	1.802	7.006	7.084	1.044
	$20Gyr$	-0.719	3.713	4.734	1.788	7.008	6.875	0.973
0.5	$10Gyr$	-1.166	3.642	4.817	2.007	6.961	8.346	1.379
	$20Gyr$	-1.116	3.647	4.787	2.097	6.980	8.187	1.341
0.4	$10Gyr$	-1.484	3.616	4.934	1.963	6.913	9.370	1.596
	$20Gyr$	-1.466	3.617	4.920	2.010	6.920	9.317	1.589
0.35	$10Gyr$	-1.602	3.609	4.966	1.942	6.888	9.729	1.652
	$20Gyr$	-1.598	3.610	4.966	1.940	6.890	9.709	1.644
0.30	$10Gyr$	-1.716	3.604	4.994	2.010	6.863	10.051	1.686
	$20Gyr$	-1.717	3.603	4.991	2.012	6.865	10.065	1.696
0.25	$10Gyr$	-1.882	3.596	5.048	2.130	6.844	10.530	1.744
	$20Gyr$	-1.866	3.596	5.032	2.110	6.840	10.490	1.744
0.20	$10Gyr$	-2.094	3.584	5.115	2.281	6.812	11.155	1.828
	$20Gyr$	-2.069	3.585	5.094	2.250	6.808	11.085	1.821
0.15	$10Gyr$	-2.394	3.564	5.210	2.482	6.759	12.066	1.970
	$20Gyr$	-2.377	3.565	5.197	2.465	6.761	12.015	1.962
0.10	$10Gyr$	-3.004	3.499	5.384	2.821	6.621	14.322	2.598
	$20Gyr$	-2.990	3.501	5.378	2.814	6.625	14.258	2.573
0.097	$10Gyr$	-3.099	3.485	5.410	2.867	6.599	14.779	2.783
	$20Gyr$	-3.084	3.488	5.407	2.860	6.603	14.691	2.740
0.095	$10Gyr$	-3.178	3.473	5.432	2.902	6.580	15.210	2.962
	$20Gyr$	-3.162	3.475	5.424	2.895	6.585	15.120	2.928
0.093	$10Gyr$	-3.281	3.456	5.458	2.949	6.555	15.879	3.251
	$20Gyr$	-3.263	3.460	5.456	2.940	6.560	15.744	3.181

This comparison is shown in Fig. 5 for both the quoted values of metallicity. For the larger masses in the sample one finds a good, and, sometime, an excellent agreement. However, going toward lower masses DM96 models appear progressively hotter until, below about $0.12M_\odot$, the disagreement is eventually reduced and sometime reversed. To discuss the origin of such a behavior, let us notice that DM96 use a similar, but not identical, treatment of the atmosphere. According to their indication, the atmosphere integration is stopped at τ=2/3 in all cases, without investigating the onset of convection. However, numerical experiments performed adopting DM96 procedure show that in that assumptions our models became "cooler", as expected from the evidence that similar models allow larger temperature

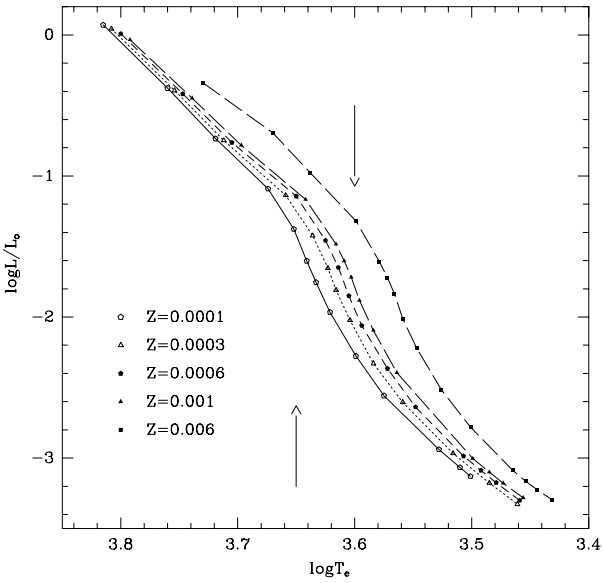

Fig. 4. The HR diagram location of the 10 Gyr old models for the assumed metallicities Z=0.0001, 0.0003, 0.0006 and 0.001. Masses of the models as reported in Tables 2 to 5 with the addition of $0.7M_\odot$ and $0.8M_\odot$ structures. The tentative location of the sequence with Z=0.006 is also reported (see text).

gradient in the atmosphere. Thus the origin of the differences is probably to be found either in the adopted EOS or in the not complete coverage of opacity tables reported by DM96. Since both papers adopt quite similar procedures to evaluate bolometric corrections and V-I color, the difference in the theoretical HR diagram are plainly transferred into the (M_V,V-I) CM diagram disclosed by Fig. 6. As for the general shape of the low main sequence, it appears that the two results differ in the sense of DM result foreseeing a larger slope of the branch below M $\approx$ $0.4M_\odot$. Note that both sequences in present paper or in DM96 keep, hopefully, full validity only for temperature larger or of the order of $\log T_e \approx 3.65$, cooler models being affected by a not-appropriate treatment of the atmosphere, overestimating the effective temperature of the stars. An estimate of such an effect can be obtained on the basis of the discussion given in Baraffe et al. (1995) for the solar metallicity. According to these Authors, it appears that the use of a $T(\tau)$ relation sizably affects the main sequence models between about $logT_e$ 3.42 and 3.58, with a maximum effect at $logT_e$ = 3.52 where the Eddington approximation produce models hotter than about $200K$. However, we lack similar indication for the metal poor models we are dealing with. Thus let us directly compare present results with recent observations of low main sequence stars. Hubble Space Telescope observation of the galactic globular cluster NGC6397, as recently presented by Paresce, De Marchi & Romaniello (1995) and by Cool, Piotto & King (1995), already disclosed a tight sequence of cluster VLM stars which represents a new fundamental test for the theory of VLM structures. According to the current literature, the metallicity of this cluster is evaluated around $[Fe/H] = -2.0$ (Webbink 1985) whereas evidences have been reported for a reddening in the range $E(B-V) = 0.15 \div 0.20$

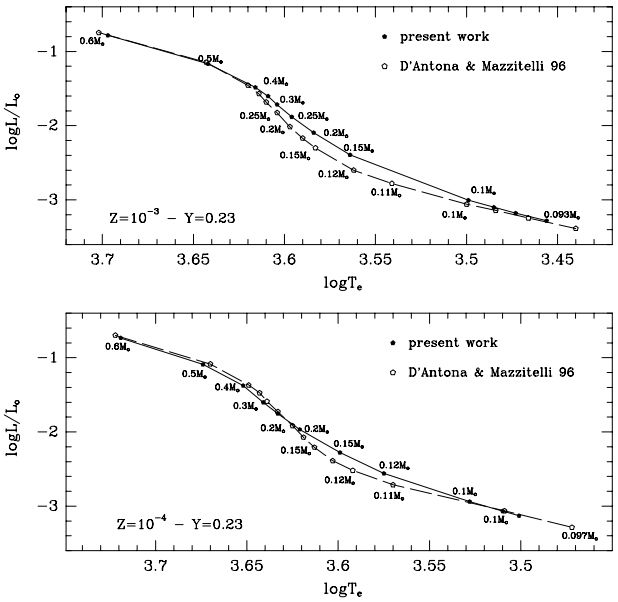

Fig. 5. Comparison of locations in the theoretical HR diagram of the 10 Gyr old models from present paper and from D'Antona & Mazzitelli (1996). Metallicity as labeled.

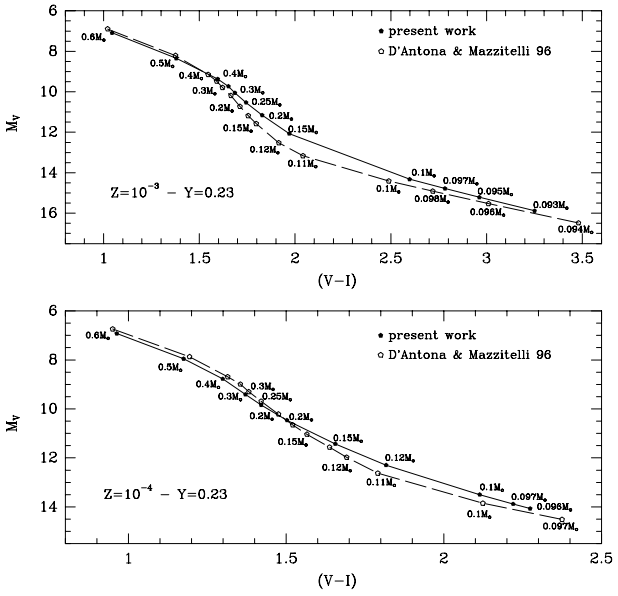

Fig. 6. Comparison of predicted distribution in the (M_V, V-I) CM diagram of the 10 Gyr old models from present paper and from D'Antona & Mazzitelli. Metallicity as labeled.

(Alcaino et al. 1987) and for a visual distance modulus ranging from 12.5 (Alcaino et al. 1987) to 12.3 (Fahlman et al. 1989). Adopting from Taylor (1986) $E(V-I) = 1.36 \times E(B-V)$, $E(V-I) = 0.20 \div 0.27$ is obtained. Fig. 7 shows the observational HST/WFPC2 data for NGC 6397 by Cool, Piotto & King (1995) as mapped in the (V,V-I) plane according to Holtzman et al. (1995) prescriptions. The same Fig. 7 shows our best fitting with theoretical (V,V-I) data, as obtained assuming for the cluster a distance modulus $(m-M)_V = 12.4$ and $E(V-I) = 0.19$, a couple of values which appear compatible with the quoted evaluations. The agreement of theoretical predictions for Z=0.0003 ($[Fe/H]$=-1.91) with the observed distribution of cluster stars can be obviously regarded as largely satisfactory. It may be noticed that the agreement has been achieved for a value of metallicity only marginally larger than expected on observational ground, without invoking the α-enhancement required by DM96 to reconcile their theoretical results with the observation. However, a more detailed discussion will be possible as soon as the effect of the $T(\tau)$ will be better understood and improved theoretical color-T_{eff} transformations (Allard 1996) suitable for metal poor stellar structures will become available.

5. VLM with known parallaxes

The fairly rich sample of stars with known parallaxes has represented for long time a valuable observational evidence constraining the theoretical approach to VLM structures. Fig. 8 shows the most complete CM diagram for similar objects presently available, as obtained adding recent data by Dahn et al. (1995) to the previous sample by Monet et al (1992). As it has been often suggested, the sequence of stars on the cooler edge of the observed distribution should be interpreted as the sequence of VLM stars with solar metallicity, with the additional evidence for metal poor subdwarfs spread in the hotter portion of the HR diagram. Recent results by Baraffe et al. (1995) support such a belief, disclosing that the color-magnitude location of $[M/H]$=-1.5 VLM structures appear in good agreement with the location of the subdwarfs in the Monet et al. (1992) sample.

As shown in the same figure, present theoretical evaluations appear in excellent agreement with such a scenario. Metal poor sequences, which represent a reasonable lower limit for the metallicity of halo subdwarfs rank indeed along the hotter boundary of the observed distribution. According to such a scenario, it has to be noticed that the CM diagram location of VLM stars appears as a metallicity indicator of unusual sensitivity, possibly to be used to investigate the metallicity distribution of stars around the Sun when the complete sample of parallaxes expected from the Hipparcos mission will be available.

As for solar metallicity VLM models, according to the results by Baraffe et al. (1995) and to the discussion given in the previous section, one expects that the treatment of the atmosphere should affect the MS location in the range 2.2 < (V-I) < 3, namely for masses in the range 0.6 < M/M$_\odot$ < 0.2. Thus, contrarily to the low metallicity case, solar metallicity models adopting $T(\tau)$ relation should give a reliable picture for the extreme lower portion of the MS only. This is partially supported by data shown by Fig. 9, where we compare the recent computations presented by Baraffe et al. (1995) with our computations for solar metallicity stars, as based just on the same zero metal EOS by Saumon & Chabrier (1992) and Saumon, Chabrier & Van Horn (1995). The same figure shows the location of the similar set of computations recently presented by D'Antona & Mazzitelli (1994,1996). In all cases, theoretical sequences have been transferred into the (M_V,V-I) CM diagram

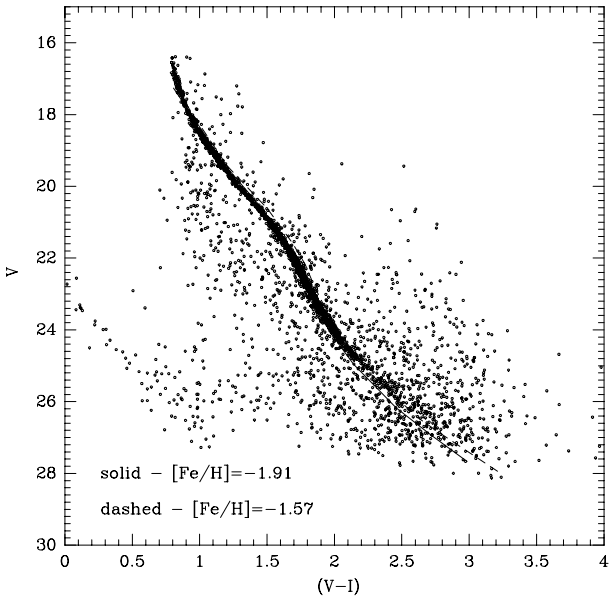

Fig. 7. (V, V-I) CM diagram for lower main sequence stars in the globular cluster NGC6397 (Cool, Piotto & King 1995). The comparison with theoretical sequences for t=10 Gyr and for the two labeled assumptions about the star metallicity has been performed adopting for the cluster $(m - M)_V$ = 12.4, $E(V - I)$ = 0.19 (see text)

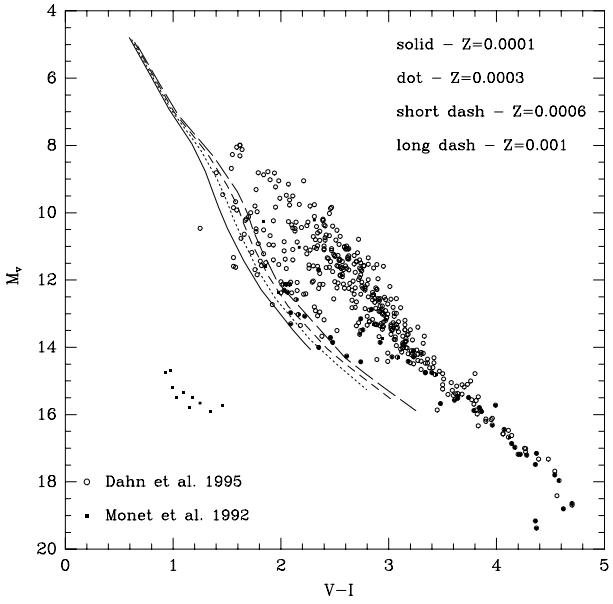

Fig. 8. (M_V,V-I) CM diagram for faint stars with known parallaxes from Monet et al. (1992) and Dahn et al. (1995) with superimposed theoretical distributions from the present paper for the labeled values of stellar metallicity.

by adopting the results of the new grid of model atmospheres given by Allard et al.(1996) for solar metallicities only. As a whole, Fig. 9 reconfirm, as repeatedly stated in the current literature, that an accurate treatment of stellar envelopes appears a necessary ingredient to produce reliable models of the upper portion of the low main sequence of metal rich stars. However, the same figure shows that both Baraffe et al. (1995) and present computations fail in accurately reproducing the location of the lowest MS masses. As pointed out by our unknown referee, this suggests that understanding VLM structures is not complete yet, and remains a tantalizing goal. As a final point, Fig. 9 discloses that present computations, when compared with DM, sensitively move the expected location of metal rich models, computed by integrating a $T(\tau)$ relation, toward observational data. The origin of such improvement is not clear. It obviously resides either in the adopted opacity or in the EOS, if not both, with only a minor influence of the adopted transformation between theoretical and observational parameters. However, it appears difficult to understand if one out of these two physical ingredients may play a major role. Nor it is known if the error in the Magni & Mazzitelli (1979) EOS, found by Saumon (1994) and discussed in DM96 could have been of relevance for these models firstly presented in D'Antona & Mazzitelli (1994).

6. Discussion and conclusions

As very recently stated in the paper by Baraffe et al. (1995), till recent times the theoretical framework for VLM stars appeared far from being satisfactory, "all the existing theoretical models failing to reproduce the observed magnitude-color diagram for the faintest objects, predicting temperature that are too large for a given luminosity". As a matter of fact, the history of VLM models is the history of the continuous decrease of model effective temperatures driven by the continuous improvement in the evaluation of the input physics (see, e.g. Dorman et al. 1989). In this context, solar metallicity models appear as the most difficult objects to be theoretically reproduced, just because of the difficult task of taking into the right account the proper influence of metals on both opacity and EOS.

Numerical experiments (Ciacio 1994) as well as inspection of the results already appeared in the literature, show that the treatment of the atmosphere or the improved physical inputs mainly affect the stellar temperature, with only a minor influence on the model luminosity. As a consequence, it could be suggested that theoretical mass-luminosity relations should have reached a reasonable degree of reliability. However, recently Chabrier et al. (1996) have emphasized the need to use accurate boundary conditions (nongray model atmospheres) between the atmosphere and the interior structure to derive more reliable mass - luminosity relationship. Nevertheless, one has to notice that not negligible differences still exist between different sets of model atmospheres (Bessel 1995, Chabrier et al. 1996) due mainly to the different methods adopted in the opacity calculations (straight-mean approximation *versus* opacity-sampling technique). In Fig. 10, we compare theoretical predictions from the present paper, by Baraffe et al. (1995) and by Chabrier et al. (1996) with observational data by Henry & McCarthy (1993). It is worth noting that our models are in good agreement with the observations and also with the theoretical mass-luminosity relation by Chabrier et al. (1996) obtained adopting the most accurate model atmospheres (Allard et al. 1996, Brett 1995)

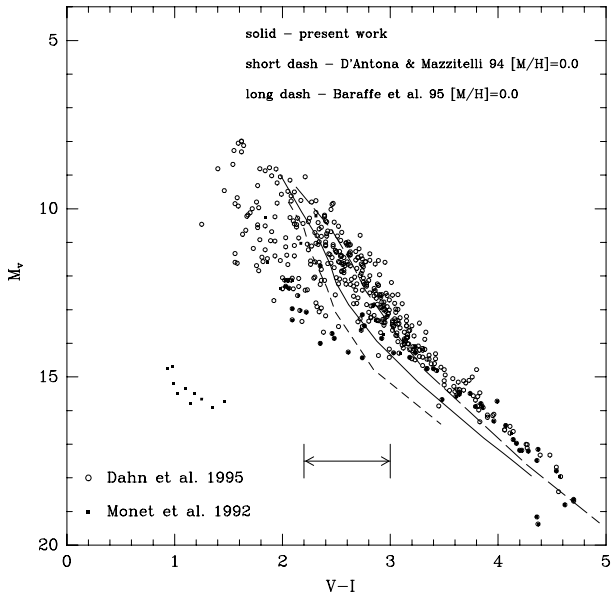

Fig. 9. (M_V,V-I) CM diagram for faint stars with known parallaxes from Monet et al. (1992) and Dahn et al. (1995) with superimposed our theoretical distributions for VLM stars of solar composition computed with the zero metal EOS of Saumon & Chabrier (1992), the theoretical models presented by Baraffe et. al. (1995) and the theoretical models of D'Antona & Mazzitelli (1994,1996).

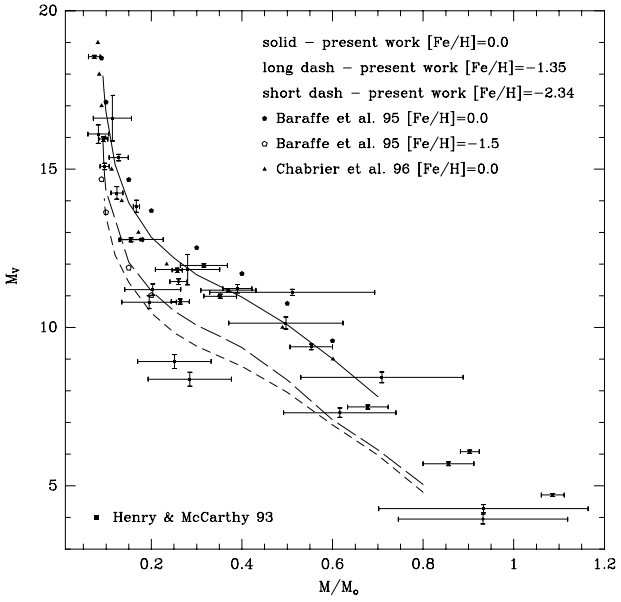

Fig. 10. Mass-luminosity relations for VLM objects for the labeled assumptions on the star metallicity, as obtained in this work (lines), by Baraffe et al. (1995) and by Chabrier et al. (1996). Observational data are from Henry & McCarthy (1993).

presently available. This evidence reinforces the suggestion, given in the previous sections, that the use of a $T(\tau)$ relation in computing stellar models has to be regarded as a first order but not-too-bad approximation to the expected evolutionary behavior. This result is, of course, a very important point since the mass - luminosity relation is at the basis of the significant problems concerning the investigation of the initial mass function in galactic globular clusters and, more in general, in stellar systems.

Acknowledgements. We gratefully acknowledge the many people whose kind cooperation allowed the completion of this work. In particular, we thank our anonymous referee for his stringent criticisms helping us to be less optimistic in approaching the problem of VLM structures. We are deeply indebted with F.Allard for providing us with the new color-temperature relation for solar metallicity, with G.Chabrier for providing his zero metal EOS, with C.C. Dahn for making available his data for dwarfs and, last but not least, with Ivan King, G. Piotto and A. Cool for allowing the use of the splendid HST data for NGC6397. S.C. warmly thanks O. Straniero and J. Fernandes for stimulating discussion on this issue.

References

Alcaino G., Buonanno R., Caloi V., Castellani V., Corsi C.E. Iannicola G. & Liller W. 1987, AJ 94, 917.
Alexander D. R., Johnson H. R., & Rypma R. L. 1983, ApJ 272, 773
Alexander D. R., Augason G. C., & Johnson H. R. 1989, ApJ 345, 1014
Alexander D.R. & Ferguson J.W. 1994, ApJ 437, 879
Allard F. 1996, *private comunication*
Allard F., Alexander D.R., Hauschildt P.H. & Schweitzer A. 1996, ApJ *submitted to*
Allard F. & Hauschildt P.H. 1995, ApJ 445, 433
Baraffe I., Chabrier G., Allard F. & Hauschildt P.H. 1995, ApJ 446, L35
Bessel M.S. 1995, in Proceedings of the ESO workshop "The bottom of the Main Sequence and Beyond", ed. Tinney C.G., p.123
Brett J.M. 1995, A&A 295, 736
Burrows A., Hubbard W.B. & Lunine J.I. 1989, ApJ 345, 939
Burrows A., Hubbard W.B., Saumon D. & Lunine J.I. 1993, ApJ 406, 158
Castellani V. 1979, ESA/Eso Workshop "Astronomical Uses of the Space Telescope", eds. F.Macchetto, F.Pacini & M. Tarenghi, p.157
Castellani V., Chieffi A. & Pulone L. 1989, ApJS 76, 911
Castellani V., Degl'Innocenti S. & Romaniello M. 1994, ApJ 423, 266
Chabrier G., Baraffe I. & Plez B. 1996, ApJ 459, L91
Ciacio F. 1994, Graduate Thesis, University of Pisa
Cool A.M., Piotto G. & King I.R. 1995, ApJ *submitted to*
D'Antona F. & Mazzitelli I. 1994, ApJS 90, 467
D'Antona F. & Mazzitelli I. 1996, ApJ 456, 329
Dahn C.C., Liebert J., Harris H.C. & Guetter H.H. 1995, in Proceedings of the ESO workshop "The bottom of the Main Sequence and Beyond", ed. Tinney C.G., p.239
Dorman B., Nelson L.A. & Chau W. J. 1989, ApJ 342, 1003
Fahlman G.G., Richer H.B., Searle L. & Thompson I.B. 1989, ApJ 343, L49
Grevesse N. 1991, in "Evolution of stars: the photospheric abundance connection", IAU Symp. eds. Michaud G., Tutukov A., p.63
Henry T.O. & McCarthy D.W. Jr, 1993, AJ 106, 773
Holtzman J.A., Burrows C.J., Casertano S., Hester J.J., Trauger J.T., Watson A.M. & Worthey G. 1995, PASP 107, 1065
Hubbard W.B. 1994, in "The Equation of State in Astrophysics", IAU Symp n.147, eds Chabrier G., Schatzman E., p.443
Huebner W.F., Merts A.L., Magee N.H. & Argo M.F. 1977, Los Alamos Sci. Lab. Rept. LA-6760-M
Krishna-Swamy K.S. 1966, ApJ 145, 174

Kurucz R.L. 1993, CD-ROM 13 and CD-ROM 18
Limber D.N. 1958, ApJ 127, 387
Magni G. & Mazzitelli I. 1979, A&A 72, 134
Monet D.G., Dahan C.C., Vrba F.J., Harris H.C., Pier J.R., Luginbuhl C.B. & Ables H.D. 1992, AJ 103, 638
Paresce F., De Marchi G. & Romaniello M. 1995, ApJ 440, 216
Rogers F.J., Iglesias C.A. 1992, ApJS 79, 507
Saumon D. 1994, in "in "The Equation of State in Astrophysics", IAU Symp n.147, eds Chabrier G., Schatzman E., p.306
Saumon D., Bergeron P., Lumine L.I., Hubbard W.B. & Burrows A. 1994, ApJ 424, 333
Saumon D. & Chabrier G. 1992, Phys.Rev.A. 46, 2084
Saumon D., Chabrier G. & Van Horn H.M. 1995, ApJS 99, 713
Taylor B.J. 1986, ApJS 60, 577
Vanderberg D.A., Hartwick F.D.A. & Dawson P. 1983, ApJ 266, 747
Webbink R.F. 1985, in "Dynamic of Star Clusters", IAU Symp. n.113, eds. Goodman J., Hut P., p.541

This article was processed by the author using Springer-Verlag LaTeX A&A style file *L-AA* version 3.